Supplement of Atmos. Chem. Phys., 18, 15145–15168, 2018
https://doi.org/10.5194/acp-18-15145-2018-supplement

Atmospheric Chemistry and Physics
Open Access
EGU

Supplement of

Quantifying uncertainties from mobile-laboratory-derived emissions of well pads using inverse Gaussian methods

Dana R. Caulton et al.

Correspondence to: Mark A. Zondlo (mzondlo@princeton.edu)

Supplemental

Figure S1. Controlled release site schematic.

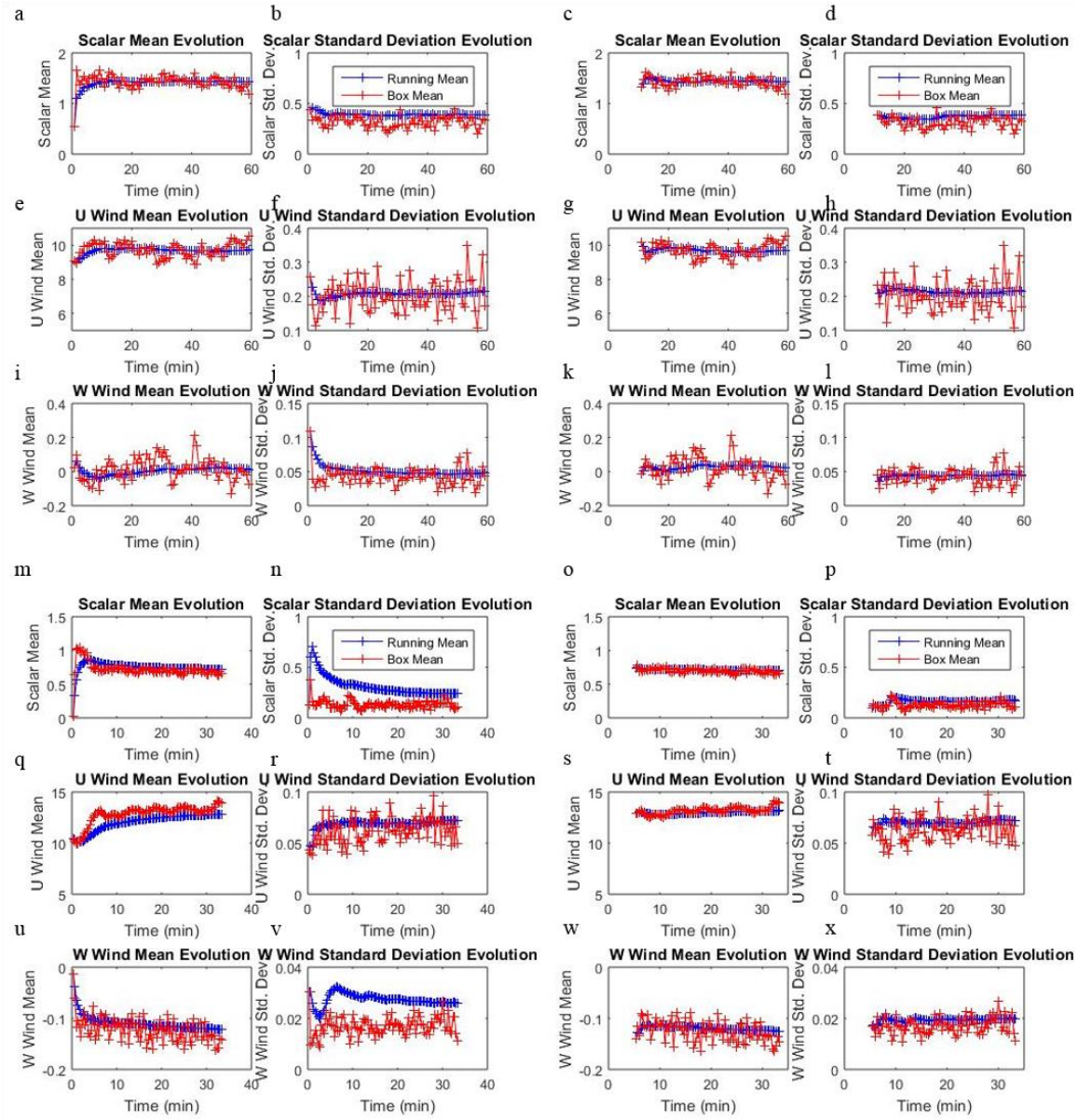

Figure S2. Comparison of box-means or standard deviations (red) and running means or standard deviations (blue) for (a-l) Site 1 and (m-x) Site 2. Left-hand panels show both sites from start-up and right-hand panels are screened to show results after a steady-state has been achieved. The running mean in the screened results starts at the determined onset of steady state.

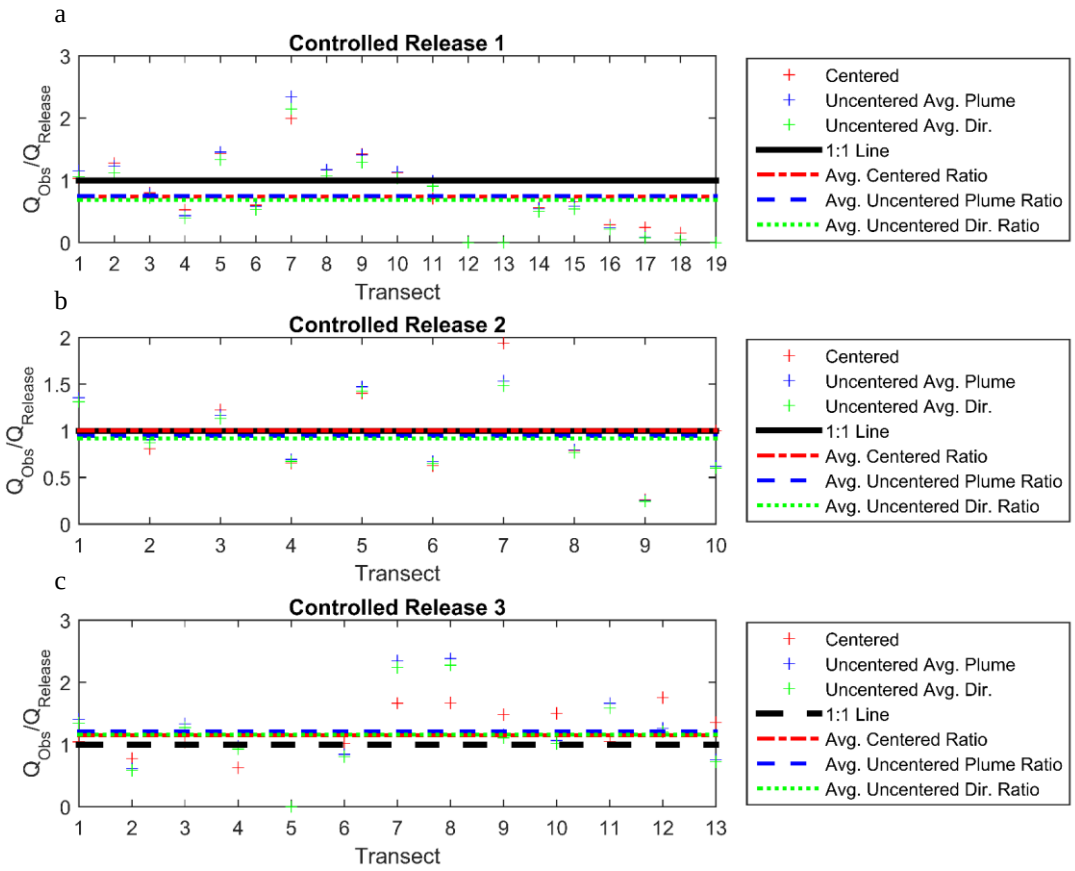

Figure S3. A comparison of release experiments 1-3 (a-c) results using the Gaussian aligned to the observation peaks (Centered) and the average Gaussian (Uncentered Avg. Plume) and the single Gaussian in the average wind direction (Uncentered Avg. Dir.).

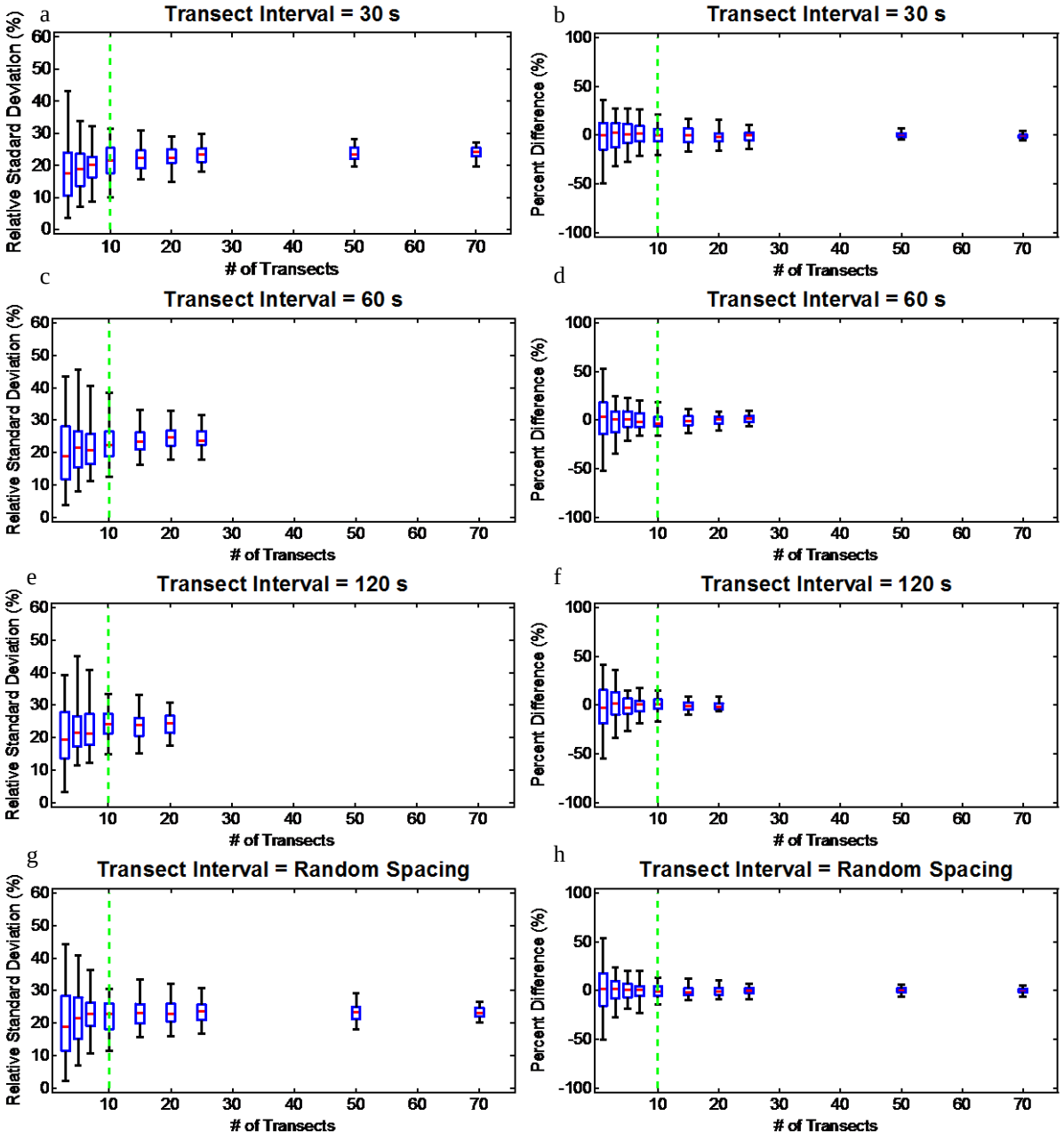

Figure S4. The rsd (a,c,e,g) of the emission retrieval using and the percent difference (b,d,f,h) between emission retrieval and known simulation emission rate using various amounts of transects and 30 second (a,b), 1 minute (c,d), 2 minute (e,f) or random (g,h) transect spacing. Box and whiskers plots show the 50th percentile (red), 25th and 75th percentile (blue) and 2.5 and 97.5 percentile (black). The recommended 10 transect criteria is shown in green.

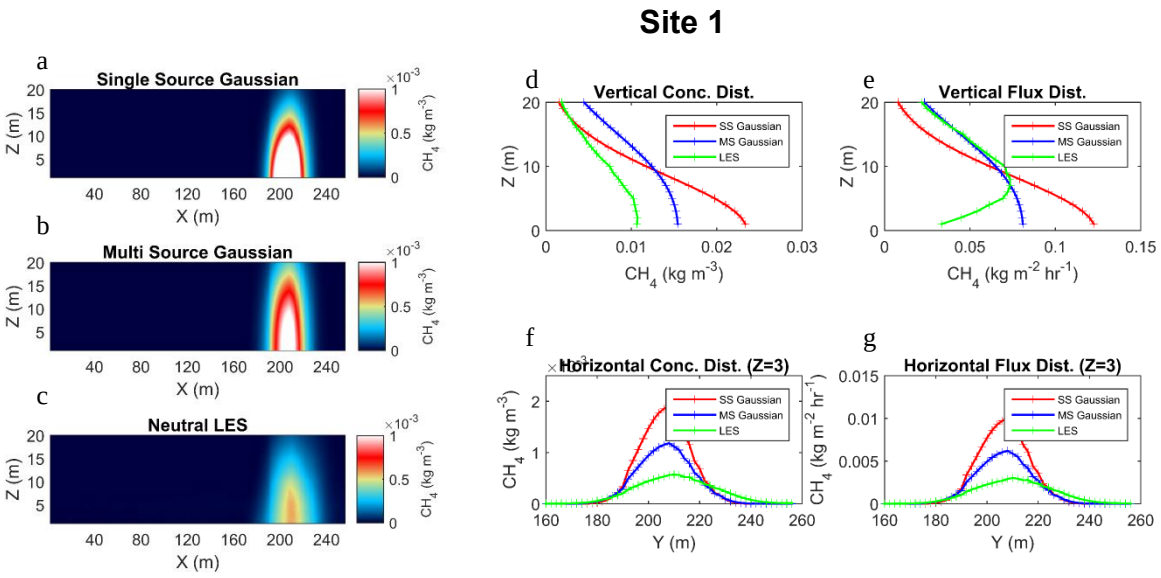

Figure S5. Comparison of three scenarios for Site 1 showing images of (a) single Gaussian, (b) multi-source Gaussian and (c) averaged LES. The comparison of vertical distributions (d) concentrations and (e) fluxes, and horizontal distributions of (f) concentrations and (g) fluxes are also shown.

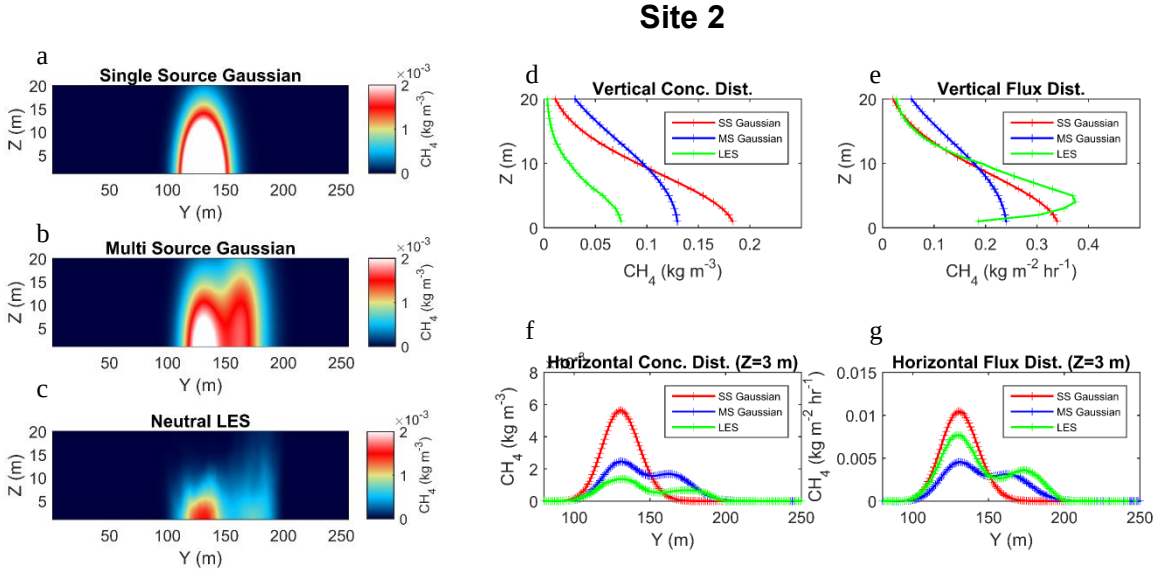

Figure S6. Comparison of three scenarios for Site 2 showing images of (a) single Gaussian, (b) multi-source Gaussian and (c) averaged LES. The comparison of vertical distributions of (d) concentrations and (e) fluxes, and horizontal distributions of (f) concentrations and (g) fluxes are also shown.

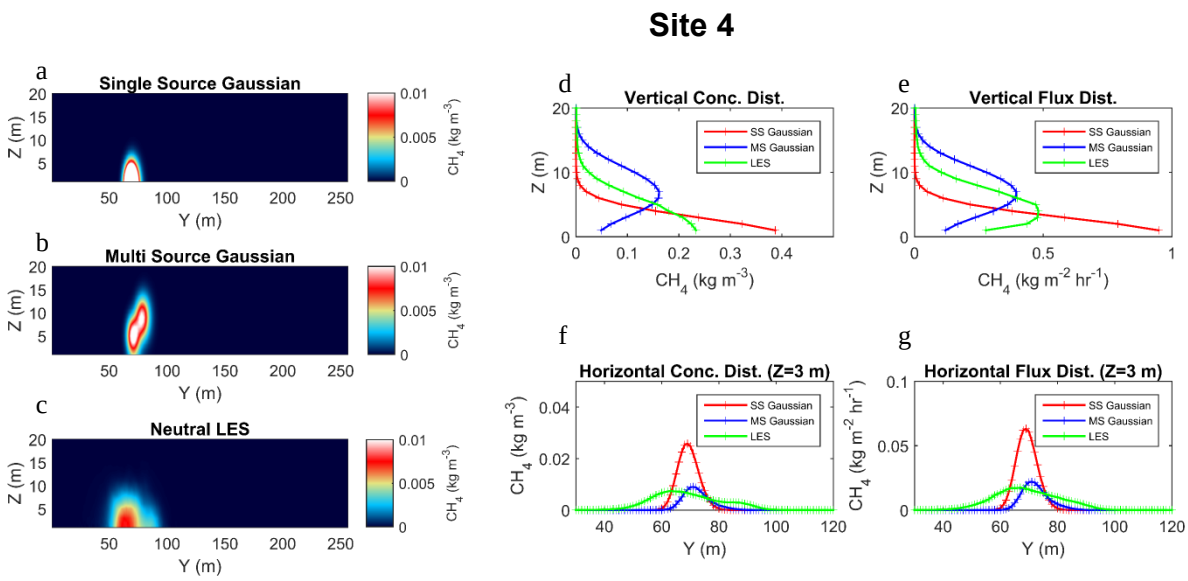

Figure S7. Comparison of three scenarios for Site 4 showing images of (a) single Gaussian, (b) multi-source Gaussian and (c) averaged LES. The comparison of vertical distributions of (d) concentrations and (e) fluxes, and horizontal distributions of (f) concentrations and (g) fluxes are also shown.

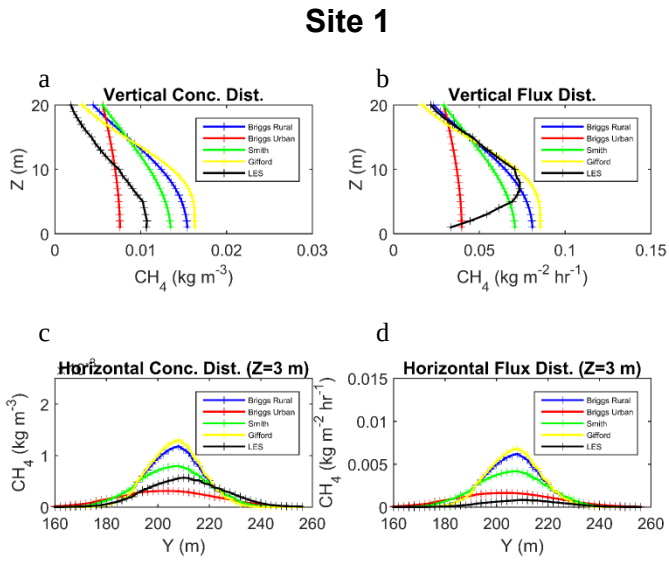

Figure S8. Comparison of scenarios using different diffusion models for Site 1 showing images of the comparison of vertical distributions of (a) concentration, (b) flux and of the horizontal distributions of (c) concentration and (d) flux.

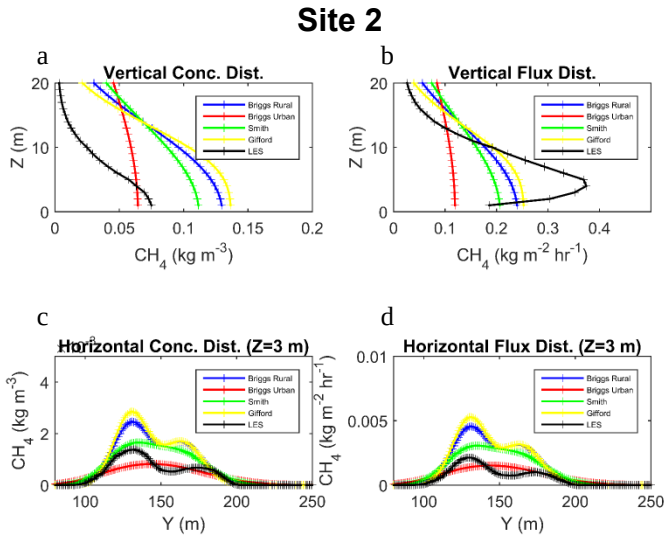

Figure S9. Comparison of scenarios using different diffusion models for Site 2 showing images of the comparison of vertical distributions of (a) concentration, (b) flux and of the horizontal distributions of (c) concentration and (d) flux.

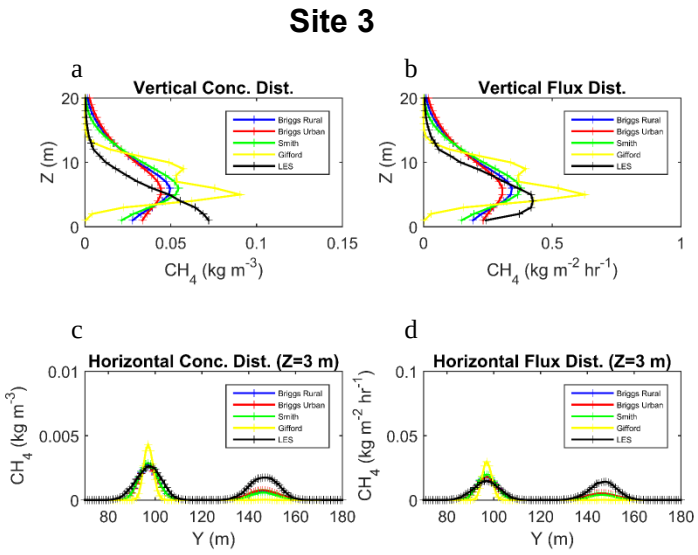

Figure S10. Comparison of scenarios using different diffusion models for Site 3 showing images of the comparison of vertical distributions of (a) concentration, (b) flux and of the horizontal distributions of (c) concentration and (d) flux.

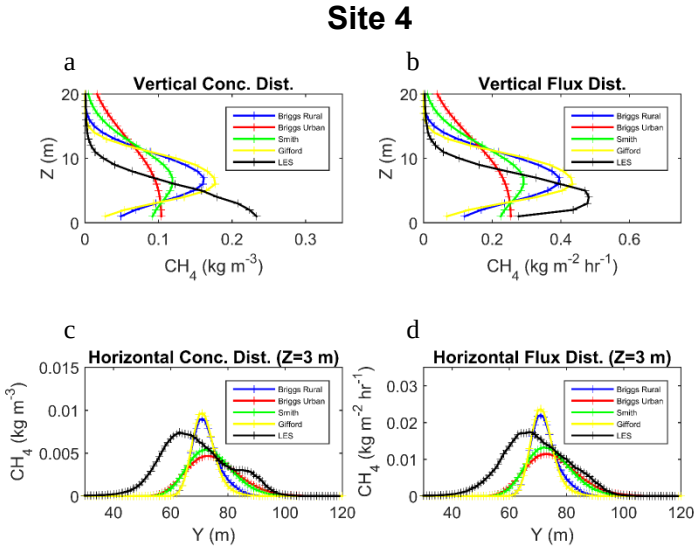

Figure S11. Comparison of scenarios using different diffusion models for Site 4 showing images of the comparison of vertical distributions of (a) concentration, (b) flux and of the horizontal distributions of (c) concentration and (d) flux.

5

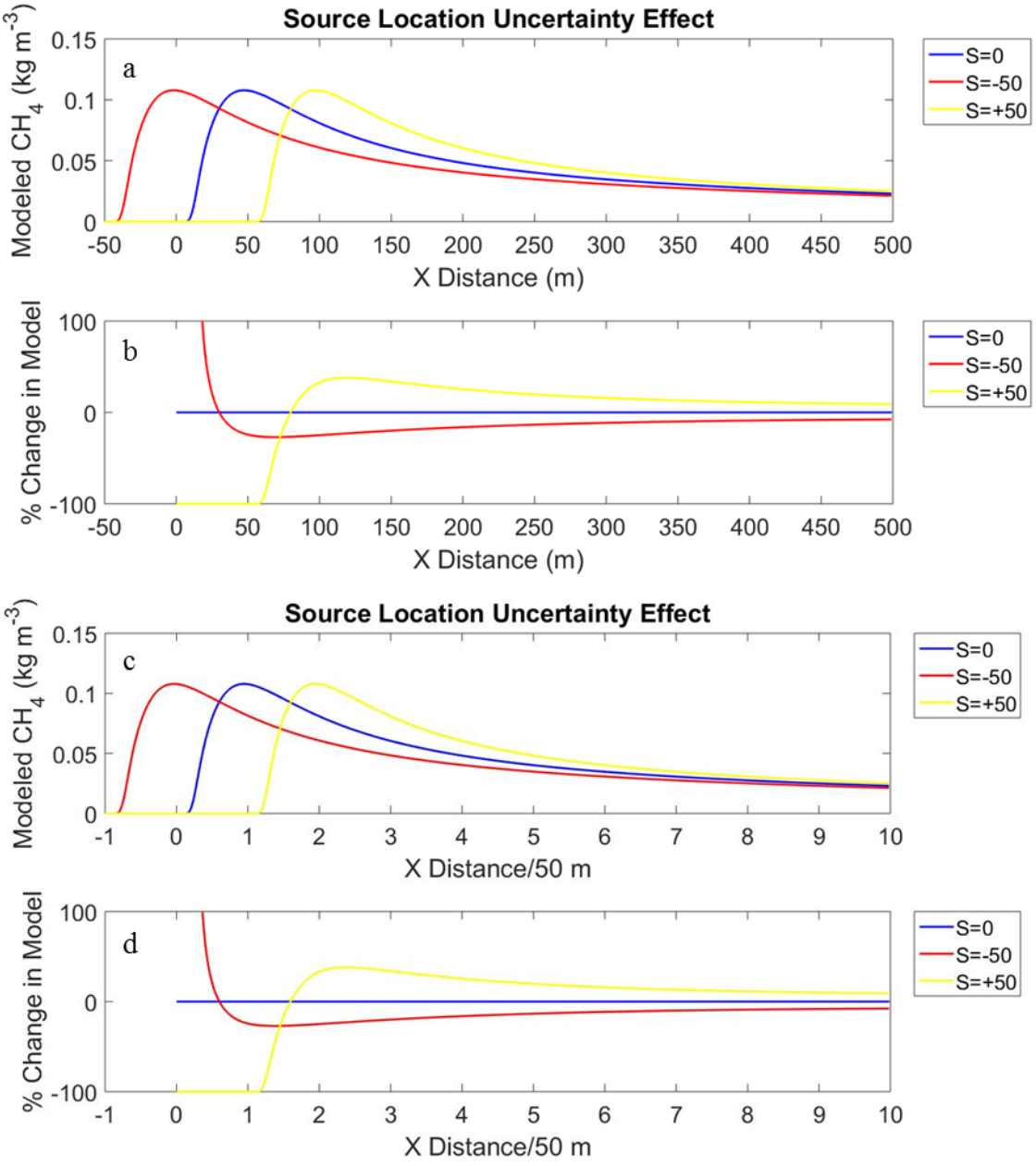

Figure S12. (a) Modeled CH_4 at three source locations at different downwind x positions assuming 3 m receptor height, 1 m source height, neutral stability and 1.5 m s^{-1} wind speed. (b) Change in % of the modeled CH_4 in each of the scenarios and base scenario (S=0). (c) The same as panel (a), normalized by the perturbation distance of 50 m. (d) The same as panel (b), normalized by the perturbation distance of 50 m.

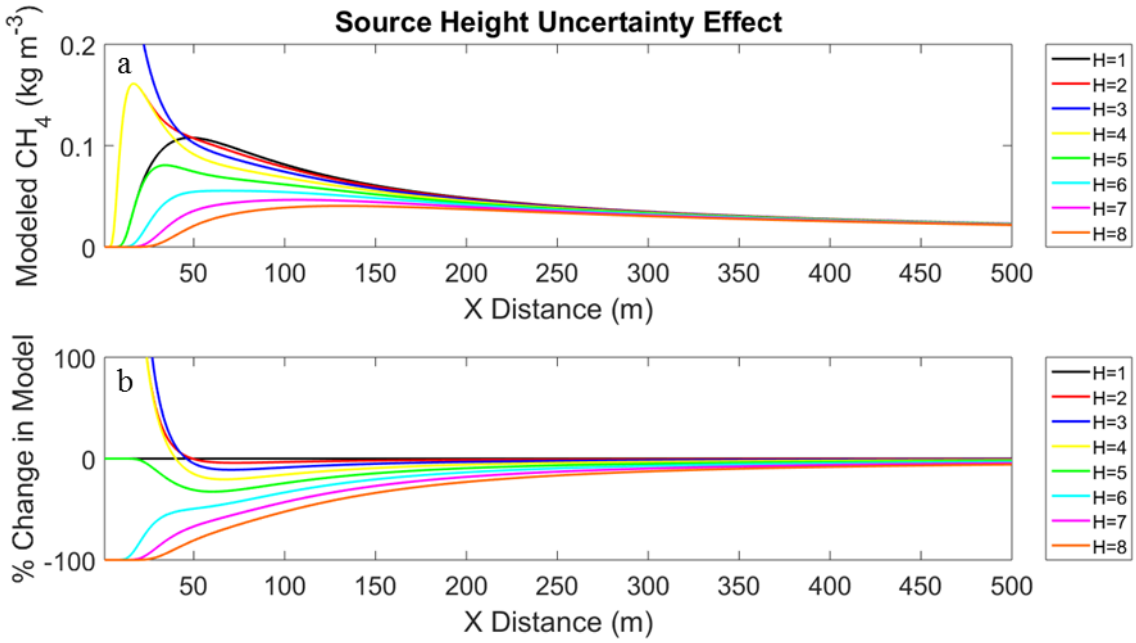

Figure S13. (a) Modeled CH_4 using 8 source heights assuming 3 m receptor height, neutral stability, and 1.5 m s^{-1} wind speed. (b) Change in % between the modeled CH_4 for each of the scenarios and the base scenario (h=1 m).

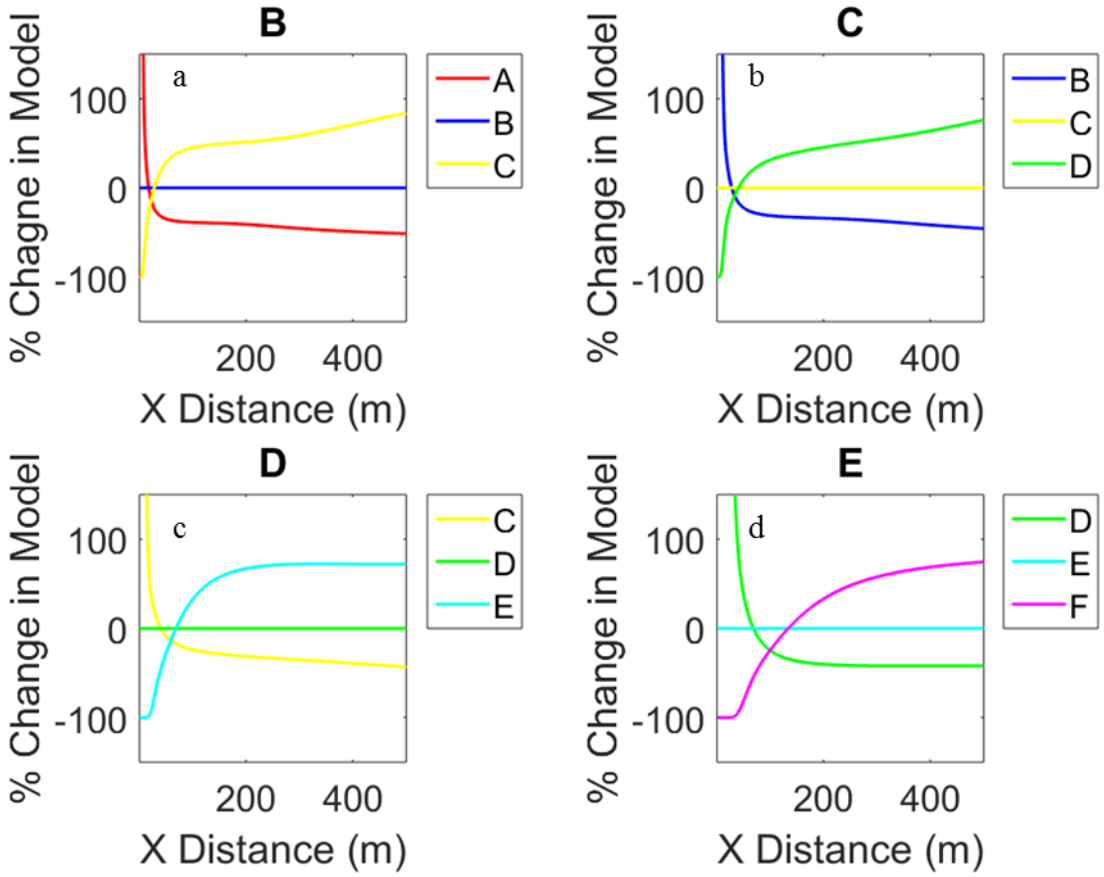

Figure S14. Change in percent between modeled CH_4 between +/- one stability class and base scenario for (a) Class B, (b) Class C, (c) Class D, and (d) Class E assuming 3 m receptor height, 1 m source height, and 1.5 m s^{-1} wind speed.

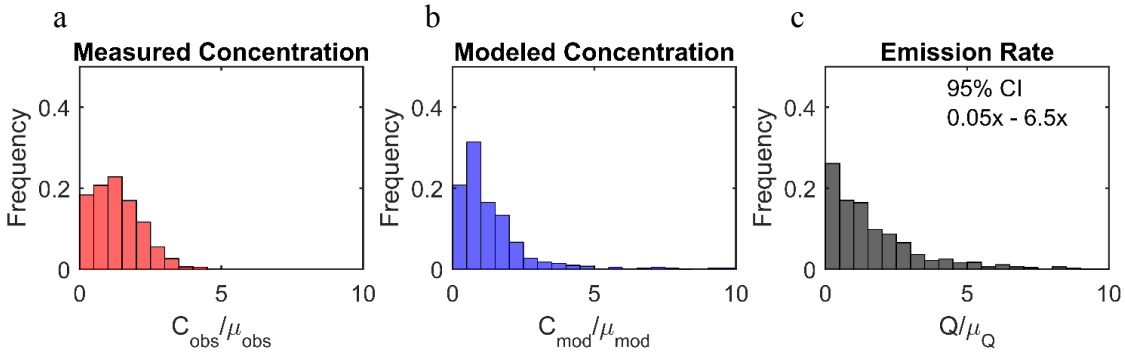

Figure S15. Monte Carlo simulations using 1,000 replicates for the standard sampling, 1 transect case showing (a) normalized observation distribution, (b) normalized model distribution and (c) normalized emission rate distribution.